Rev. Roum. Sci. Techn.– Électrotechn. et Énerg.
Vol. 71, 3, pp. 403–408, Bucarest, 2026

HYBRID CONTROL FOR MAXIMUM POWER EXTRACTION AND VOLTAGE STABILITY IN PHOTOVOLTAIC-BATTERY SYSTEMS

MAHMOOD AMEEN THABIT[1*], KAMEL S. BELKHIR[1], LAKHDAR MADANI[1], HOUCEM ACHOURI[1], ALA ADDIN ALDWA[2]

Keywords: Photovoltaic; Battery storage system; Maximum power point tracking; Backstepping control; Stability; Microgrid.

Photovoltaic power systems face two main challenges: inefficient power extraction under variations in irradiance and temperature, and DC bus voltage instability due to power mismatches. This paper outlines the development, modeling, and simulation of a standalone PV system with battery storage and DC-DC converters, employing a hybrid control strategy that simultaneously addresses these critical challenges. Maximum power point tracking is applied to enhance energy extraction from the PV array under perturbation conditions. A backstepping controller ensures accurate PV voltage tracking and maintains system stability under varying operating conditions. Moreover, to sustain the required constant DC bus voltage, a proportional–integral controller regulates battery charging and discharging. The proposed system is evaluated in MATLAB/Simulink under standard conditions to assess static stability and under varying irradiation, temperature, and load conditions to test the dynamic stability. A simulation study was conducted, and the results confirm improved power extraction and enhanced voltage stability, demonstrating the effectiveness of the proposed approach for DC microgrid applications.

1. INTRODUCTION

Photovoltaic (PV) energy has become increasingly popular for sustainable electricity generation. PV cells can convert sunlight into usable electrical energy, making them useful in rural regions without access to the electrical grid [1].

A significant challenge in standalone PV systems is their inability to efficiently extract and regulate solar energy, as their performance is highly influenced by weather conditions such as irradiation fluctuations and temperature variations. This can affect the system's ability to supply continuous energy [2,3]. Additionally, standalone PV systems experience DC bus voltage fluctuations due to mismatches between generation and demand. To address this problem, storage systems are added to PV systems. These systems store excess energy generated during peak sunlight hours for later use during low-light hours. Designing and controlling such systems is often challenging due to the need to balance performance with operational cost constraints. Therefore, effectively managing the energy exchange between the PV system, the battery, and the load remains a significant challenge, requiring a strategy to optimize both maximum power extraction and stable voltage regulation in real time [4].

This paper details the design and simulation of a standalone PV system combined with battery storage and a bidirectional DC-DC converter. Simulations are performed using MATLAB. This system is tested under standard testing conditions (STC) as well as during changes in irradiation, temperature, and load demand.

The rest of this paper is organized as follows: Section 2 describes the system architecture with PV, battery storage, and bidirectional buck-boost converter modeling. Section 3 describes the control strategies, which include maximum power point tracking (MPPT), backstepping, and PI controllers. In Section 4, the simulation results and analysis are presented. In Section 5, the paper is concluded with an overview of the results and recommendations for further research.

2. DESCRIPTION AND MODELING OF THE SYSTEM

The mathematical modeling of each PV system component is presented in the following section. Fig. 1 shows the system's general structure, which includes the management of the generated power delivered to the load. It includes a DC-DC boost converter that allows harvesting the maximum power from the solar panel while maintaining a constant output capacitor voltage. Additionally, this enables MPPT control by ensuring robust operation of the photovoltaic panel despite changing environmental conditions.

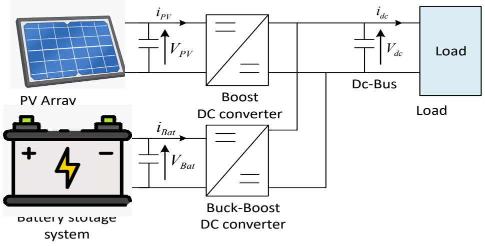

Fig. 1 – Structure of the standalone PV-battery power system.

2.1 PV CELL MODELING

A photovoltaic panel consists of many electronic cells, and the PV module is the main source of energy, as it converts solar radiation into electrical power. The PV array is modeled using a single-diode model, one of the most popular due to its accuracy and simplicity in PV array simulation [5]. The equivalent circuit of the one-diode model is shown in Fig. 2, which consists of a current source, a diode, a series resistance R_s , and a shunt resistance R_{sh}.

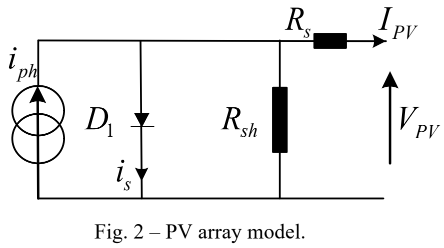

Fig. 2 – PV array model.

The mathematical model of the PV cell that determines the output current I_{PV} of a PV cell is expressed by [6]:

$$I_{PV} = I_{ph} - I_s\left[e^{q\frac{V_{PV}+R_S I_{pv}}{nKT_k}} - 1\right] - \frac{V_{PV} + R_s I_{pv}}{R_{sh}}, \quad (1)$$

where V_{PV} is the voltage at the PV array, I_{ph} is the photocurrent generated by solar irradiance, I_s is the diode reverse saturation current, q is the electron charge, n is the diode ideality factor, K is the Boltzmann constant, T_k is the cell temperature in Kelvin.

[1] LSI Laboratory, Department of Electrical Engineering, Faculty of Technology, Setif 1 University – Ferhat Abbas, Algeria.
E-mail: mahmood.thabit@univ-setif.dz*, ksbelkhir@univ-setif.dz, lakhdar.madani@univ-setif.dz, achouri.houssam@univ-setif.dz,
[2] Electrical engineering Laboratory, Electrical engineering department, Faculty of Technology, University of M'sila, M'sila Algeria.
E-mail: Aldawah.alaa@univ-msila.dz

DOI: 10.59277/RRST-EE.2026.3.11

2.2 MODELING OF THE DC–DC BOOST CONVERTER

The main objective of the control strategy is to stabilize the PV output voltage and ensure it reaches the desired MPPT reference value. To achieve this, the boost converter must be accurately modeled. This model describes the relationship between the converter's parameters, as described by the following [7]:

$$\frac{\mathrm{d}V_{PV}}{\mathrm{d}t} = \frac{1}{C_{PV}}(i_{PV} - i_L), \tag{2}$$

$$\frac{\mathrm{d}i_L}{\mathrm{d}t} = \frac{1}{L}\left[-Ri_L + V_{pv} - (1-\mu)V_{dc}\right], \tag{3}$$

where L is the inductance of the boost converter, V_{dc} is the output voltage, and μ is the duty cycle. The PV capacitor C_{pv}, boost inductor L, and series resistance R are key system parameters that determine the converter dynamics.

2.3 MODELING OF THE BATTERY STORAGE SYSTEM

An autonomous photovoltaic system incorporates a battery storage system to help mitigate the variability issues associated with solar energy. The battery is modeled using the equivalent circuit model, which comprises an open-circuit voltage V_{oc}, an internal resistance R_{int}, and a state of charge SOC [8]. The battery voltage V_{bat} is then given by:

$$V_{bat} = V_{oc} - I_{bat}R_{int}. \tag{4}$$

The SOC capacity of the battery is estimated using the Coulomb counting method [9,10] with the following equation:

$$SOC = SOC_{init} - \frac{1}{C_{bat}}\int I_{bat}\mathrm{d}t\,, \tag{5}$$

where SOC_{init} is the initial state of charge of the battery, and C_{bat} is the nominal battery capacity.

2.4 MODELING OF THE DC-DC BIDIRECTIONAL CONVERTER

The bidirectional buck-boost converter manages energy flow between the battery and the DC bus, operating in charging and discharging modes to maintain a stable DC bus voltage and ensure efficient energy utilization. This controller regulates the converter's duty cycle to maintain the system's stability and provide a constant bus voltage [11]. When the photovoltaic array cannot meet the load demand, the converter operates in boost mode to raise the battery voltage V_{bat} to the DC bus voltage, allowing the battery to power the load. The input–output voltage relationship can be given by:

$$V_{dc} = \frac{V_{bat}}{(1-d_{bat})}, \tag{6}$$

where d_{bat} is the duty cycle of the converter, and the relationship between the voltages is:

$$V_{bat} = d_{bat}V_{dc}. \tag{7}$$

This dual function allows the converter to smoothly switch between charging and discharging while maintaining a stable DC bus voltage [12].

3. **DESCRIPTION OF THE STUDIED CONTROL TECHNIQUE**

The designed combined control strategy integrates the perturb and observe (P&O) MPPT algorithm, backstepping control, and a PI controller to ensure optimal system performance. This algorithm determines the reference voltage $V_{pv_{ref}}$ for maximum power extraction. The backstepping control regulates the boost converter to ensure that the V_{pv} tracks $V_{pv_{ref}}$, while the PI controller works with the backstepping controller to regulate the V_{dc} voltage, starting with controlling the bidirectional buck-boost, and ensuring that the battery compensates for fluctuations in PV power output. Fig. 3 illustrates the control process.

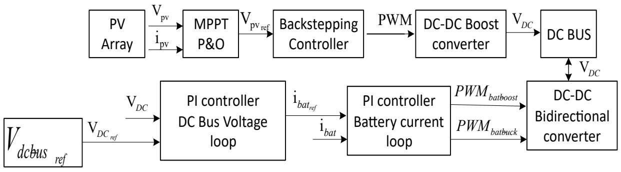

Fig. 3 – Scheme of the control technique.

3.1 TECHNIQUE OF PERTURB AND OBSERVE CONTROL (P&O):

The P&O technique is used to maximize power extraction from the PV array due to its simplicity and ease of implementation. It adjusts the PV voltage and monitors the resulting change in power output to ensure the PV system operates at its maximum power point even under varying environmental conditions. The algorithm derives the ideal reference voltage V_{dc} dynamically [13, 14]. Mathematically, the P&O MPPT logic follows these rules:

$$V_{PV_{ref}} = V_{PV_{ref}} + \Delta V\text{ , if : } P_{pv} \rightarrow \text{increases}, \tag{8}$$

$$V_{PV_{ref}} = V_{PV_{ref}} - \Delta V\text{ , if : } P_{pv} \rightarrow \text{decreases}. \tag{9}$$

Figure 4 shows the flowchart of the P&O algorithm, which starts by measuring the PV voltage V_{pv} and its power, then perturbs the PV voltage by small steps and tries to determine an adjusted $V_{pv_{(i+1)}}$ [15].

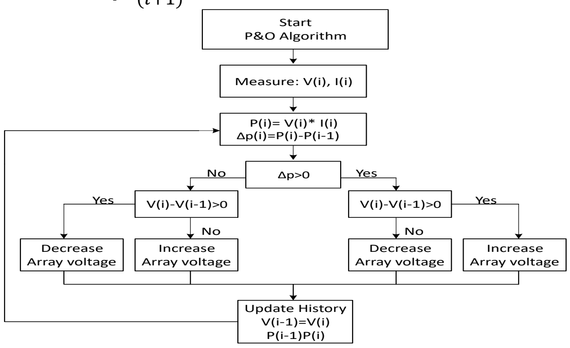

Fig. 4 – P&O algorithm.

3.2 BACKSTEPPING CONTROLLER

The backstepping control technique is used in our system to ensure that the PV voltage accurately follows the reference voltage provided by the P&O MPPT algorithm. This nonlinear control method improves system stability and robustness, particularly under changing environmental conditions. It works by defining voltage and current tracking errors and systematically designing control laws using Lyapunov stability theory. The voltage loop ensures V_{pv} that $V_{pv_{ref}}$, while the current loop regulates the inductor current, generating the appropriate duty cycle for the boost converter [16,17]. Their mathematical equations are studied in the following steps, starting by defining the voltage tracking error e_1:

$$e_1 = V_{pv} - V_{pv_{ref}}. \tag{10}$$

By substituting the boost converter model, to ensure V_{pv}

follows $V_{pv_{ref}}$, the obtained equation becomes:

$$e_1^* = \frac{1}{C_{pv}}\left(i_{pv} - i_L\right) - V_{pv_{ref}}^*. \quad (11)$$

Then, a Lyapunov candidate function V_1 is chosen as:

$$V_1 = \frac{1}{2}e_1^2. \quad (12)$$

By deriving V_1 with respect to time:

$$V_1^* = e_1 e_1^*, \quad (13)$$

while knowing that $e_1^* = -K_1 e_1$, using K_1 the backstepping gain for the voltage loop, the candidate function derivative becomes:

$$V_1^* = K_1 e_1^2. \quad (14)$$

Substituting e_1^* from the PV dynamics to ensure ($V_1^* \le 0$) achieving stability for voltage tracking:

$$\frac{1}{C_{pv}}\left(i_{pv} - i_L\right) - V_{Pv_{ref}}^* = K_1 e_1. \quad (15)$$

By determining $\alpha = i_{L_{ref}}$ where α is the function of stabilization, we finally get the $i_{L_{ref}}$ expression:

$$\alpha = i_{PV} - C_{PV}\left(V_{Pv_{ref}}^* + K_1 e_1\right). \quad (16)$$

A second error variable e_2 for the inductor current is defined as:

$$e_2 = i_L - \alpha, \quad (17)$$

derivative:

$$e_2^* = i_L^* - \alpha^*. \quad (18)$$

After that, a second Lyapunov function V_2 can be defined as:

$$V_2 = V_1 + \tfrac{1}{2}e_2^2, \quad (19)$$

derivative:

$$V_2^* = e_1 e_1^* + e_2 e_2^*, \quad (20)$$

The derivative of the second error can be calculated as:

$$e_2^* = \frac{1}{L}\left[V_{pv} - (1-\mu)V_{dc} - Ri_L\right] - \alpha^*. \quad (21)$$

The following equations are determined using (13), (14), and (15) to ensure the stability of the system:

$$e_1^* = \frac{1}{C_{pv}}i_{pv} - \frac{e_2}{C_{pv}} - \frac{\alpha}{C_{pv}} - V_{pv_{ref}}^*, \quad (22)$$

$$e_1^* = -K_1 e_1 - \frac{e_2}{C_{pv}}, \quad (23)$$

$$V_1^* = -K_1 e_1^2 - \frac{e_1 e_2}{C_{pv}}. \quad (24)$$

Since $e_2^* = -K_2 e_2^*$using K_2 the backstepping gain for the current loop, and to ensure the system remains stable and errors converge to zero when($V_2 \le 0$):

$$V_2^* = -K_1 K_1^2 - K_2 K_2^2 \le 0. \quad (25)$$

The backstepping controller derives μ to ensure both errors e_1 e_2 converge to zero [18],

$$-K_2 e_2 = \frac{1}{L}\left[V_{pv} - (1-\mu) - V_{dc} - Ri_L\right] - \alpha^* - \frac{e_1}{C_{pv}}. \quad (26)$$

Therefore, the final control law for the duty cycle μ:

$$\mu = 1 - \frac{1}{V_{dc}}\left(-Ri_L + V_{pv} + LK_2 e_2 - L\alpha^* - \frac{Le_1}{C_{pv}}\right). \quad (27)$$

3.3 PI CONTROLLER

The PI controller regulates the DC bus voltage by controlling the battery charging and discharging through the bidirectional buck–boost converter. It first computes the DC voltage error. The error is then processed by the PI controller to produce a reference battery current that stabilizes the bus voltage [19,20]. The voltage error e is calculated as follows:

$$e = V_{dc_{ref}} - V_{dc}. \quad (28)$$

Then, the PI control law to determine the battery current reference that is necessary to keep the DC bus voltage stable can be defined as:

$$I_{bat_{ref}} = K_{pv}e + K_{iv}\int e\mathrm{d}t\,, \quad (29)$$

where K_p and K_i are the proportional and integral gains of the PI controller. The battery current error is calculated to ensure that the battery current matches the desired reference current:

$$e_{bat} = I_{bat_{ref}} - I_{bat}. \quad (30)$$

Then we calculate the duty cycle for a bidirectional Buck-Boost converter that manages battery charging and discharging as

$$d_{bat} = K_{pi}e_{bat} + K_{ii}\int e_{bat}\mathrm{d}t\,. \quad (31)$$

To control the dynamic response of the DC bus voltage, we apply the following equation that determines the relationship between DC bus voltage V_{dc} and battery current I_{bat}:

$$C_{dc}\frac{\mathrm{d}V_{dc}}{\mathrm{d}t} = I_{Load} - I_{bat}, \quad (32)$$

where C_{dc} is the DC bus capacitance, and I_{Load} is the load current.

4. SIMULATION AND RESULTS

To evaluate the performance of the standalone PV-battery system, we conducted simulations in MATLAB/Simulink under different conditions. (Simulink models can be made available upon request. The system consists of a PV array, a battery, a boost converter, and a bidirectional buck-boost converter. The P&O MPPT algorithm generates the reference PV voltage $V_{pv_{ref}}$, which is tracked by the backstepping controller. Additionally, the PI controller manages the battery's charging and discharging process and maintains a stable DC bus voltage.

The following table specifies the system parameters, including PV array specifications, battery characteristics, and converter components:

Table 1

Characteristics of the PV-battery system

Parameter	Value
Series strings	4
Parallel strings	1
Cells per module	36
Input Capacitance	63 μF
Inductor	3 mH
PV capacitor	63 μF
DC bus capacitor	200 μF
Battery type	Lithium-Ion
Number of batteries	3
Nominal voltage of batteries	24V
Buck- Boost Inductor	3mH
Backstepping voltage-loop control gain K1	3300
Backstepping current-loop control gain K2	11800
Proportional gain of PI controllerK_{pv}, K_{pi}	0.124, 7.275
Integral gain of PI controllerK_{iv}, K_{ii}	1.414, 2000
Sample Time T_{sv},T_{si}	500e-6, 50e-6

The PV-battery standalone system was tested under two primary scenarios to evaluate its performance and stability: static stability under normal conditions and dynamic stability under weather changes and variable power demands. The P&O MPPT Backstepping-PI controller operated together to extract the maximum power, regulate the PV and DC bus voltages, and manage the battery's charging and discharging efficiently, ensuring a stable and reliable energy supply.

4.1 STATIC STABILITY TEST: NORMAL CONDITIONS

In this case, the system was evaluated under standard test conditions, where the irradiance is constant (1000W/m²), constant temperature (25°C), and the load is resistive and set to (320 Ω). This scenario was used as a critical evaluation to verify the system's and control strategy's stability under ideal operating conditions.

PV VOLTAGE TRACKING PERFORMANCE

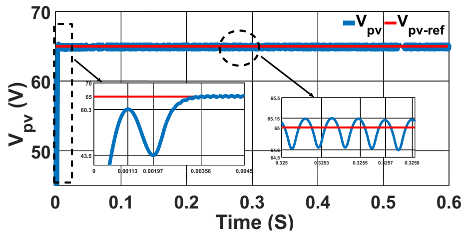

Fig. 5 – PV voltage tracking performance under standard conditions.

Figure 5 presents the PV voltage V_{pv} response compared to the reference voltage $V_{pv_{ref}}$. The results indicate that the backstepping controller successfully tracks the reference voltage with high accuracy, demonstrating the system's ability to track the MPP and achieve steady-state stability within 0.004s with minimal transient response. This confirms the effectiveness of the P&O MPPT-based backstepping approach in maintaining optimal operating conditions and indicates excellent static stability and fast convergence to the desired operating point

DC BUS VOLTAGE REGULATION

To maintain a stable DC bus voltage, the system was designed to provide a constant and steady voltage to the load. Figure 6 compares the actual DC bus voltage V_{dc} with its reference value $V_{dc_{ref}}$, demonstrating how well the system maintains stability across different operating conditions.

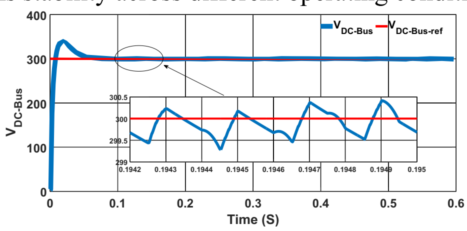

Fig. 6 – DC bus voltage response under standard conditions.

As shown in Fig. 6, the DC bus voltage V_{dc} closely follows the reference voltage, consistently maintaining a stable output of 300V. This highlights the bidirectional buck-boost converter's effectiveness in regulating the DC bus voltage under static conditions, thereby ensuring a highly stable DC bus voltage.

BATTERY CHARGE-DISCHARGE STATIC

Figure 7 shows the battery charging and energy storage performance by comparing the battery current with its reference:

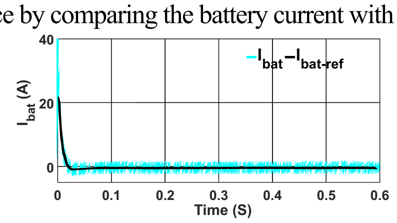

Fig. 7 – Battery current tracking under standard conditions.

The battery current I_{bat} successfully tracks the $I_{bat_{ref}}$ current that comes from the controller, indicating that the system effectively manages the battery's charge and discharge cycles, as shown by the stable I_{bat} curve.

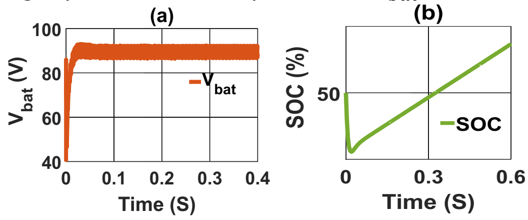

Fig. 8 – Battery voltage and state of charge under standard conditions.

The battery smoothly absorbs excess PV power, as reflected in the state of charge (SOC) curve, Fig. 8b, which shows a gradual increase in stored energy. The battery voltage in Fig. 8a remains within a stable range, confirming the efficiency of the charge controller in managing battery charging under normal conditions.

4.2 DYNAMIC STABILITY TEST: PERTURBATION CONDITIONS

In this case, the system was subjected to variable irradiation, temperature, and load changes to evaluate its dynamic stability. The chosen irradiance range (300–1000 W/m²) and temperature range (18–35°C) represent typical operating conditions encountered in standalone photovoltaic systems, while the transitions between resistive, inductive, and capacitive loads simulate changes in practical load demand. This test, therefore, represents realistic operating scenarios, including changes in solar irradiance due to passing clouds or weather fluctuations, to assess the adaptability and dynamic performance of the proposed system. The corresponding variations in irradiance, temperature, and load are presented in Fig. 9.

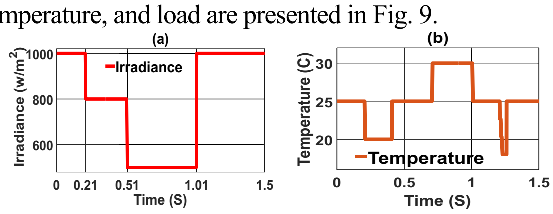

Fig. 9 – Profile of the variable level of irradiance and temperature.

Figure 9 illustrates the varying irradiation and temperature levels used in the simulation. The irradiation starts at 1000 W/m², drops to 800 W/m², then further decreases to 500 W/m², and fluctuates between 300 and 800 W/m². On the other hand, the temperature varies between 25, 18, 35, and 25°C. These changes test how well the system can maintain controlled stability and optimal performance under dynamic environmental conditions.

PV VOLTAGE TRACKING UNDER PERTURBATIONS

Figure 10 shows the system's response to perturbations, such as variations in irradiation, temperature, and load conditions. The load profile alternated between resistive, inductive, and capacitive loads.

Minor deviations occur during irradiation changes, but the system quickly returns to steady state, demonstrating robust dynamic stability. Temperature variations have a negligible impact, while inductive and capacitive loads cause slight perturbations. However, the system recovers rapidly, maintaining accurate tracking of the reference voltage.

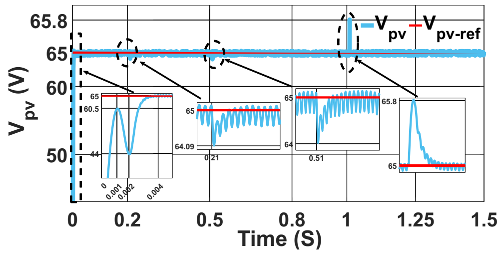

Fig. 10 – PV voltage behavior during disturbance.

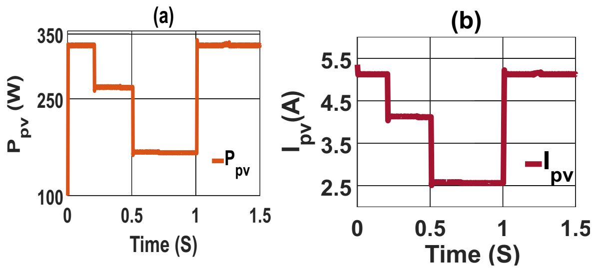

Fig. 11 – PV power and current behavior during disturbance.

Figure 11 shows the PV power and current responses under perturbation conditions. Despite environmental and load variations, PV power and current I_{pv} curves in both figures remain stable. The system dynamically adapts to changes, ensuring continuous MPPT operation, demonstrating the effectiveness of the designed control technique under dynamic conditions.

DC BUS VOLTAGE BEHAVIOR DURING DISTURBANCE

To evaluate the system's ability to maintain a stable DC bus voltage under dynamic conditions, the DC bus voltage V_{dc} was tested under varying irradiation and load changes.

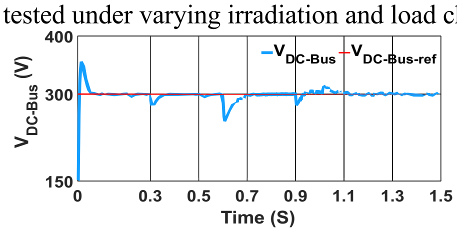

Fig. 12 – DC Bus voltage response behavior during disturbance.

Figure 12 demonstrates how V_{dc} it reacts to changes in irradiation and load compared to its reference $V_{dc_{ref}}$ under varying conditions. Each disturbance causes slight deviations in the V_{dc} curve. However, the backstepping-PI controller effectively restores stability, ensuring that the voltage quickly returns to the reference value. Inductive loads, in particular, cause the most significant transient response, but the system demonstrates robust performance by stabilizing rapidly.

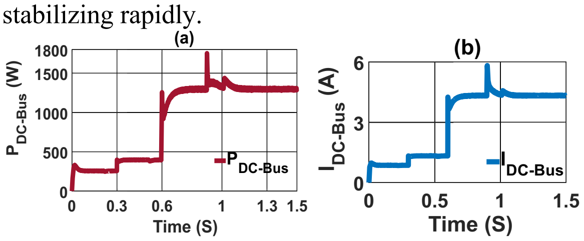

Fig. 13 – DC bus power and current behavior during disturbance.

Figure 13 shows the DC bus power P_{dc} and current I_{dc}. The curves indicate stable operation, with the system continuously adapting to maintain reliable power flow.

BATTERY CHARGE-DISCHARGE DYNAMICS

The battery current I_{bat} responds to perturbations by adjusting its charge and discharge cycles. During irradiation and load changes, the I_{bat} curve follows the reference, ensuring efficient energy management.

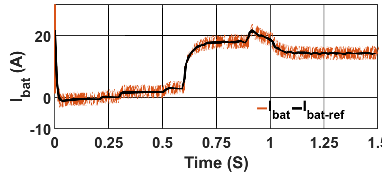

Fig. 14 – Battery current level during disturbance.

Figure 14 shows how battery operation changes in response to perturbations and how the battery current closely follows its reference, ensuring precise control of charging and discharging cycles during variations in load and irradiation. When irradiation is high, the battery stores extra energy, as shown by tracking the charging reference. During high load, the battery discharges.

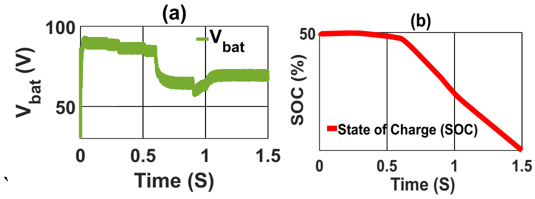

Fig. 15 – Battery voltage and state of charge during disturbance.

Figure 15 illustrates the battery's energy storage behavior. Both figures show how charging and discharging cycles are regulated to maintain an optimal charge level, ensuring the battery operates efficiently despite variations in the DC bus voltage.

4.3 COMPARATIVE STUDY WITH CONVENTIONAL CONTROLLER

In this case, the proposed P&O–Backstepping–PI controller is compared with a conventional MPPT–PI controller to evaluate the reference tracking, transient performance, and voltage regulation quality during varying conditions that are applied in case two

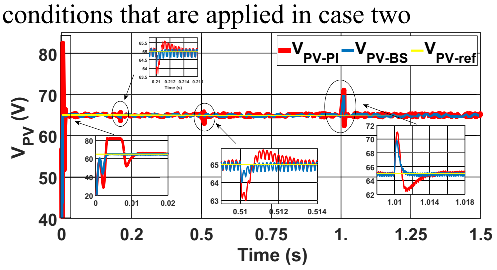

Fig. 16 – Comparison of PV voltage tracking during disturbance.

Figure 16 compares the PV voltage-tracking performance of the conventional and proposed controllers under varying operating conditions. The conventional controller shows a fluctuating transient period with significant oscillations before reaching the reference voltage, with a stabilization time of approximately 0.18s and a transient of approximately 12%. While the proposed controller clearly improves transient behavior, it reduces the stabilization time to approximately 0.05 seconds and limits the transient to approximately 3%. Moreover, the steady-state tracking error decreased from approximately 2V for the conventional controller to less than

0.5V with the proposed approach, demonstrating improved tracking accuracy and enhanced stability.

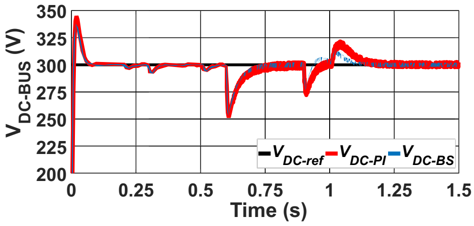

Fig. 17 – Comparison of DC voltage tracking during disturbance.

Figure 17 compares the DC bus voltage responses of both controllers. Both controllers follow the reference voltage under steady-state conditions. However, during disturbances, the conventional MPPT-PI controller exhibits a larger voltage deviation of approximately 45 V and a higher ripple of approximately 10 V under irradiance and load changes. The proposed controller significantly improves voltage regulation and quickly returns the PV voltage to the reference value, limiting deviation to approximately 15 V and reducing ripple to around 3 V. These results demonstrate that the proposed hybrid control strategy provides faster stabilization and more effective regulation of the DC bus voltage under dynamic conditions.

5. CONCLUSION

In this work, a standalone PV–battery power system was developed, and its efficiency and stability were demonstrated under both normal and dynamic environmental conditions. The traditional methods often suffer from oscillations, instability, and slow adaptation to changes in irradiance and load. To overcome these limitations, a hybrid control strategy combining P&O MPPT technology with a backstepping-PI controller was proposed. The system, controlled by this hybrid technique, showed excellent performance under varying operating conditions. The system demonstrated strong adaptability to environmental and load variations. Simulation results confirmed that the P&O MPPT–backstepping-PI controller effectively tracked the PV voltage reference, ensuring optimal power extraction from the PV array.

Meanwhile, the bidirectional boost converter maintained a constant DC bus voltage and managed battery charge and discharge cycles based on DC bus demand. The designed control technology also demonstrated robust performance under disturbances, quickly recovering from transients. Comparative results demonstrated that the P&O MPPT–backstepping-PI controller provided improved dynamic performance, faster transient response, lower oscillations, and enhanced robustness under perturbations compared to conventional controllers. making it highly suitable for standalone PV–battery systems under fluctuating conditions. Future work may include integrating wind energy sources, enhancing nonlinear control strategies, implementing advanced intelligent controls, and validating the system through real-time hardware deployment.

CREDIT AUTHORSHIP CONTRIBUTION STATEMENT

MAHMOOD AMEEN THABIT: methodology, simulation, writing, original draft.
KAMEL S. BELKHIR: supervision, review & editing, validation.
LAKHDAR MADANI: supervision, review & editing, referencing.
HOUCEM ACHOURI: simulation support, writing, system modeling.
ALA ADDIN ALDWA: simulation support, writing, control design.

Received on 3 August 2025

REFERENCES

1. P.A. Owusu, S. Asumadu-Sarkodie, "A review of renewable energy sources, sustainability issues and climate change mitigation," Cogent Engineering, **3**, *1* (2016).
2. A. Firah, M. Birane, A. Degla, "Techno-economic based optimization of photovoltaic/battery/diesel generator microgrid," Rev. Roum. Sci. Techn. – Série Électrotechnique et Énergétique, **70**, *4*, pp. 447–452 (2025).
3. H. Jiang, Y. Hou, Z. Qian et al., "Impact of climate changes on the stability of solar energy: Evidence from observations and reanalysis," Renewable Energy, **208**, pp. 726–736 (2023).
4. R. Gugulothu, B. Nagu, D. Pullaguram, "Energy management strategy for standalone DC microgrid system with photovoltaic/fuel cell/battery storage," Journal of Energy Storage, **57**, Art. 106274 (2023).
5. S.R. Pendem, S. Mikkili, "Modeling, simulation and performance analysis of solar PV array configurations (series, series–parallel and honeycomb) to extract maximum power under partial shading conditions," Energy Reports, **4**, pp. 274–287 (2018).
6. E.I. Batzelis, "Simple PV performance equations theoretically well founded on the single-diode model," IEEE Journal of Photovoltaics, **7**, *5*, pp. 1400–1409 (2017).
7. Y. Sun, H. Wang, Z. Qi, "Modelling and control of DC–DC converters," in Control of Power Electronic Converters and Systems, Academic Press, pp. 69–92 (2018).
8. M. Chen, G.A. Rincon-Mora, "Accurate electrical battery model capable of predicting runtime and I–V performance," IEEE Transactions on Energy Conversion, **21**, *2*, pp. 504–511 (2006).
9. Z. Chen, B. Xia, C.C. Mi, "A novel state-of-charge estimation method for lithium-ion battery pack of electric vehicles," in Proceedings of the 2015 IEEE Transportation Electrification Conference and Expo (ITEC), IEEE, pp. 1–6 (2015).
10. F. Calero, C.A. Cañizares, K. Bhattacharya, "Dynamic modeling of battery energy storage and applications in transmission systems," IEEE Transactions on Smart Grid, **12**, *1*, pp. 589–598 (2020).
11. L. Devarajan, S. Chellathurai, "Aquila optimized nonlinear control for DC–DC boost converter with constant power load," Rev. Roum. Sci. Techn. – Série Électrotechnique et Énergétique, **69**, *4*, pp. 419–424 (2024).
12. P.K. Sahu, S. Jena, B.C. Babu, "Power management and bus voltage control of a battery backup-based stand-alone PV system," Electrical Engineering, **104**, *2*, pp. 1097–1110 (2022).
13. N.A. Kamarzaman, C.W. Tan, "A comprehensive review of maximum power point tracking algorithms for photovoltaic systems," Renewable and Sustainable Energy Reviews, **37**, pp. 585–598 (2014).
14. M.A. Thabit, L. Madani, K.S. Belkhir, "Maximum power point tracking based on a robust backstepping control for a standalone photovoltaic system," in Proceedings of the 2024 3rd International Conference on Advanced Electrical Engineering (ICAEE), IEEE, pp. 1–6 (2024).
15. A. Harrison, A. Ambe et al., "An enhanced P&O MPPT algorithm for PV systems with fast dynamic and steady-state response under real irradiance and temperature conditions," International Journal of Photoenergy, **2022**, Art. 6009632 (2022).
16. K. Ali, Q. Khan, S. Ullah, I. Khan, L. Khan, "Nonlinear robust integral backstepping based MPPT control for stand-alone photovoltaic system," PLoS ONE, **15**, *5*, Art. e0231749 (2020).
17. A. Harrison, A. Ambe et al., "Robust nonlinear MPPT controller for PV energy systems using PSO-based integral backstepping and artificial neural network techniques," International Journal of Dynamics and Control, **12**, *5*, pp. 1598–1615 (2024).
18. G. Melath, M.N. Hussain, V. Agarwal, "A nonlinear adaptive backstepping controller for stabilizing the DC bus voltage of an islanded hybrid microgrid," IEEE Journal of Emerging and Selected Topics in Industrial Electronics, **3**, *3*, pp. 538–548 (2022).
19. M.F. Zahra, A. Chaghi, K.S. Belkhir, L. Madani, "Design of PI and backstepping controllers for distribution static compensator," in Proceedings of the 2018 International Conference on Applied Smart Systems (ICASS), IEEE, pp. 1–6 (2018).
20. K.K. Pandey et al., "Bidirectional DC–DC buck–boost converter for battery energy storage system and PV panel," in Modeling, Simulation and Optimization: Proceedings of CoMSO 2020, Springer, pp. 241–251 (2021).